Exploring the active mechanism of berberine against HCC by systematic pharmacology and experimental validation

LEI SONG[1*], YI LUO[1*], XINYUE WANG[2*], MOHAMMED M. ALMUTAIRI[3], HUAFENG PAN[1], WEIRONG LI[1], YONGQIANG LIU[1], QI WANG[1] and MING HONG[1]

[1]Institute of Clinical Pharmacology, Guangzhou University of Chinese Medicine, Guangzhou, Guangdong 510405;
[2]Sun Yat-sen University Cancer Center, Guangzhou, Guangdong 510060, P.R. China;
[3]Department of Pharmacology & Toxicology, University of Kansas, Lawrence, KS 66045, USA

Abstract. Berberine (BBR) is the main component of Coptidis rhizoma, the dried rhizome of *Coptis chinensis* and is a potential plant alkaloid used for the treatment of cancer due to its high antitumor activity. The present study examined the therapeutic potential and molecular mechanism of action of BBR against HCC, using systematic pharmacology combined with a molecular docking approach and experimental validation *in vitro*. Through systematic pharmacological analysis, it was found that BBR serves a significant role in inhibiting HCC by affecting multiple pathways, especially the PI3K/AKT signaling pathway. Furthermore, the docking approach indicated that the binding of BBR to AKT could lead to the suppression of AKT activity. The present study examined the inhibitory effect of BBR on the PI3K/AKT pathway in HCC and identified that BBR downregulated the expressions of phosphorylated AKT and PI3K in MHCC97-H and HepG2 cells, inhibiting their growth, cell migration and invasion in a dose-dependent manner. In addition, inhibition of the AKT pathway by BBR also contributed to cell apoptosis in MHCC97-H and HepG2 cells. Taken together, the results of the present study suggested that BBR may be a promising antitumor drug for HCC that acts by inhibiting the PI3K/AKT pathway.

Introduction

Hepatocellular carcinoma (HCC) is one of the most common types of cancer in humans, and in China alone accounts for 53% of all liver cancer-related deaths worldwide (1,2), representing the second most common cause of cancer-related mortalities (3). Potential therapies for HCC include local ablative therapies, liver transplantation and resection. However, these therapies are effective only for treating HCC at early stages (4). For advanced stages, systemic therapy with the tyrosine kinase inhibitor sorafenib is the best available option, as indicated by current data (5). Treatment with sorafenib presents various side effects, such as diarrhea, hypertension and skin toxicity (6). Therefore, understanding the molecular mechanisms involved in development of HCC is essential to uncover novel drugs for targeted therapies. Berberine (BBR), a natural isoquinoline alkaloid (Fig. 1), is found in the roots, rhizome and stem bark of a number of important medicinal plants (7). In the clinical setting, BBR has been used for decades to treat patients who have diarrhea (8), acute radiation intestinal syndrome (9) and type 2 diabetes mellitus (10), with doses of 0.1-0.3 g three times a day, 20 mg/kg once a day and 0.9 g once a day with negligible adverse reactions. Previous studies also have shown that BBR exhibits antitumor properties (11) against ovarian cancer (12), breast cancer (13), nasopharyngeal carcinoma (14), thyroid carcinoma (15) and prostate cancer (16), with the IC_{50} of BBR of 2.79 mg/l, 26.5 μM, 11.7 μg/ml, 125.6 and 220.36 μM, respectively. BBR has been proposed to exhibit several antitumor activities that target multiple signaling pathways, for example the PI3K/AKT pathway, that are crucial for tumor progression (17). Despite several investigations, the precise cellular and molecular targets of BBR remain unknown (18). In addition, the molecular mechanisms of action of BBR in HCC have yet to be fully elucidated. Therefore, the present study investigated the potential anti-HCC effect of BBR and examined its molecular mechanism of action using computer-aided approaches.

Computer-aided approaches have been widely used in drug research to improve the efficiency of drug discovery. Systematic pharmacology is an emerging field that combines multiple drug target prediction, oral bioavailability prediction and network analysis to understand the active compounds and therapeutic targets of Traditional Chinese medicine (TCM) (19). As a receptor-based computer-assisted drug design approach, molecular docking mainly predicts the interactions between two or several molecules based on both

---

Correspondence to: Dr Ming Hong or Dr Qi Wang, Institute of Clinical Pharmacology, Guangzhou University of Chinese Medicine, 12 Airport Road, Baiyun, Guangzhou, Guangdong 510405, P.R. China
E-mail: hongming1986@gzucm.edu.cn
E-mail: wangqi@gzucm.edu.cn

*Contributed equally

geometry and energy match (20). As for other tumors, many emerging treatments of HCC need further evaluation (5). Efforts are underway to explore the molecular mechanisms for the treatment of HCC and for the development of novel therapeutic approaches with lower toxicity. The present study provided *in vitro* experimental evidence to validate the mechanisms of action of BBR in treating HCC at the molecular level, as were predicted by systems pharmacology and molecular docking results.

Materials and methods

Evaluation of pharmacokinetic properties by TCM systems pharmacology (TCMSP). TCMSP (http://lsp.nwu.edu.cn/tcmsp.php; version 2.3) is an open-source systems pharmacology platform for TCM that provides information on the interactions among drugs, targets and diseases. This database includes herbal products, chemicals, targets, drug-target networks and drug-target-disease networks; as well as pharmacokinetic properties of natural ingredients including drug-likeness (DL), oral bioavailability (OB), fractional negative accessible surface area (FASA-), blood-brain barrier (BBB), Caco-2 permeability (Caco-2) and Lipinski's rule of five [molecular weight (MW), total polar surface area (TPSA), octanol-water partition coefficient (ALogP), H-bond donor (Hdon) and H-bond acceptor (Hacc)] (21). In the present study, the molecular name 'berberine' was searched in TCMSP and the drug-like properties of BBR were analyzed at the molecular level.

Target fishing by TCMSP and PharmMapper. The putative targets of BBR were collected from two databases, TCMSP and PharmMapper (http://www.lilab-ecust.cn/pharmmapper/; updated: April 10, 2019) (22). TCMSP is a useful analysis platform and knowledge repository. Drug-target mappings were collected from two sources in TCMSP: Experimentally validated targets were obtained from the database for Herb Ingredients' Target (http://lifecenter.sgst.cn/hit/; downloaded on July 28, 2018) and the Systems Drug Targeting (https://targetingsystems.net/; downloaded on July 30, 2018) model construction was used to predict potential targets that were not validated. Support Vector Machine score (SVM) ≥0.7 and Random Forest score (RF) ≥0.8 were set as the threshold to identify candidate targets (23). PharmMapper, a free web server, can identify potential drug targets using the pharmacophore mapping approach. A mol2 file for BBR was obtained from TCMSP database and uploaded in PharmMapper.

HCC-significant target selection. HCC-significant targets were obtained from two databases including OncoDB.HCC (http://oncodb.hcc.ibms.sinica.edu.tw/index.htm; downloaded on August 13, 2018) and Liverome (http://liverome.kobic.re.kr/; downloaded on August 14, 2018). OncoDB.HCC is a comprehensive tumor genomic database that displays abnormal cancer related target genes and loci seen in HCC (24); while Liverome is a database of genes associated with HCC. In these databases, gene signatures are mostly from proteomics studies and published microarray data manually assembled and annotated (24).

Protein-protein interaction (PPI) data. The protein-protein interaction (PPI) data were obtained from Search Tool for the Retrieval of Interacting Genes/Proteins (STRING) database (http://string-db.org/; version 10) (25), with the species limited to 'Homo sapiens'.

Gene Ontology (GO) and pathway enrichment analysis. GO and Kyoto Encyclopedia of Genes and Genomes (KEGG) pathway enrichment analysis were performed using Database for Annotation, Visualization and Integrated Discovery (DAVID; http://david.abcc.ncifcrf.gov/; version 6.8) (26,27).

Network construction and analysis. Construction of BBR-BBR targets network and PPI networks were visualized using Cytoscape (http://cytoscape.org/; version 3.6.0) (28).

Molecular docking algorithm. Before the docking process, the three-dimensional (3D) crystal structures of AKT were obtained in the PDB format from RCSB Protein Data Bank (http://www.pdb.org/; PDB-ID:3MVH; Released: June 2, 2010) and prepared with Autodock 4.2 (http://autodock.scripps.edu/;version 1.2) for flexible docking studies. The 3D structure of BBR (Pubchem CID: 2335) was obtained from NCBI-PubChem (https://pubchem.ncbi.nlm.nih.gov/), energy optimization was performed with ChemOffice (http://www.cambridgesoft.com; version 17.0) and saved in the PDB format. Gasteiger charges were added, rotatable bonds were set by the AutoDock tools and all torsions were allowed to rotate. Polar hydrogen atoms were added to the protein using AutoDock tools. The grid map was centered at the active site pocket of the protein by Autogrid (version 1.4.5) (29). The root-mean-square deviation value was less than 2.0 Å. Briefly, to perform docking in AutoDock 4.2, the grid dimensions were established using the grid center, number of points (X: 60, Y: 60, Z: 60) and spacing (0.375 Å). Molecular docking was performed and analyzed using AutoDock 4.2. A Lamarckian genetic algorithm method (Runs 100) was implemented in the program suite to identify appropriate binding modes and conformation of the ligand molecules (30). A maximum of 25 million energy evaluations were applied for the experiment. The results were clustered using a tolerance of 2.0 Å. Analysis of BBR and target protein docking results using Pymol (https://pymol.org/2/; version 2.3) and ligplot (https://www.ebi.ac.uk/thornton-srv/software/LigPlus/; version 1.4).

Cell lines, culture conditions and reagents. MHCC97-H and HepG2 cell lines were obtained from the Cell Bank of the Chinese Academy of SciencHes (Shanghai, China). The cells were cultured in DMEM (Thermo Fisher Scientific, Inc.) containing 10% heat inactivated FBS (Thermo Fisher Scientific, Inc.), 100 U/ml penicillin and 100 μg/ml streptomycin and maintained as monolayer in a humidified atmosphere of 95% air and 5% CO_2 at 37˚C. Culture medium was replaced every 2 days. BBR was purchased from Chengdu Desite Chemical Co. Ltd. and a stock solution of 10 mM was prepared in DMSO (Sigma-Aldrich; Merck KGaA). The solution was serially diluted in DMEM immediately before the experiments. Pancreatin, penicillin and streptomycin were purchased from Gibco (Thermo Fisher Scientific, Inc.). All the reagents were of analytical grade.
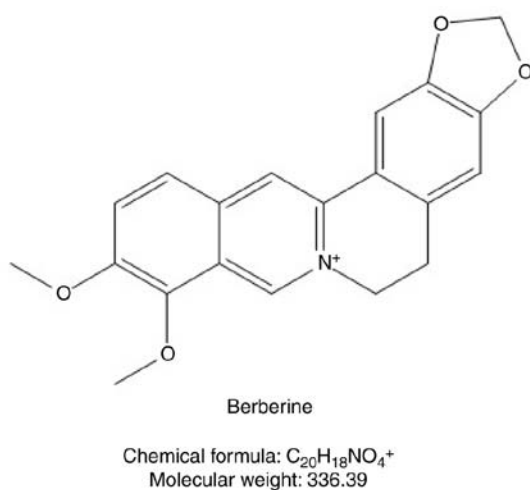
Figure 1. Structure of berberine. Chemical structure of berberine (left); and energy-minimized 3D structure of berberine (right).

Western blotting. Following treatment with different concentrations of BBR for 24 h, MHCC97-H and HepG2 cells were harvested and washed with ice-cold PBS. Total cellular protein was extracted by lysing cells in buffer containing 50% glycerol, 10% SDS, 0.5 M Tris/HCl (pH 6.8), 1:100 proteases and phosphatases inhibitor cocktail. Protein concentrations were determined using the BCA method (Beyotime Institute of Biotechnology). Then, 50 μg protein was separated by 10% SDS PAGE and transferred onto PVDF membranes (Bio-Rad Laboratories, Inc.). Membranes were blocked with 5% BSA (Gibco; Thermo Fisher Scientific, Inc.) in TBST (0.1% TWEEN) for 2 h at room temperature. The membranes were incubated overnight at 4˚C with appropriate primary antibodies including anti-PI3K p85-α (1:1,000; cat. no. ab182651; Abcam), anti-AKT (1:1,000; cat. no. 9272; Cell Signaling Technology, Inc.), anti-phosphorylated (p-) AKT (1:1,000; Cell Signaling Technology, Inc.) and β-actin (1:6,000; ab8227; Abcam). After being incubated with HRP-conjugated goat anti-rabbit (1:1,000; ab181662; Abcam) or anti-mouse IgG (1:1,000; ab205719; Abcam) for 1 h at room temperature, immune complexes were detected using enhanced chemiluminescence (ECL kit; EMD Millipore). Protein expression levels were normalized to β-actin and quantified using Image Lab software version 6.0.1 (Bio Rad Laboratories, Inc).

Cell viability assay. Cells were collected by trypsinization (GE Healthcare Life Sciences) after replacing the medium twice. The cells were cultured in 96-well plates at a density of 5×10^4 cells per well. After 24 h of incubation, cells were treated with various concentrations of BBR (50, 100 and 200 μM) and cultured for 24 h. The cells in the logarithmic growth phase were used for detecting cell viability using the MTT assay. At the end of the incubation, 10 μl of MTT solution (Sigma-Aldrich; Merck KGaA) was added to each well and incubated for another 2.5 h. DMSO (100 μl) was used to dissolve formazan crystals and absorbance was detected at wavelength of 570 nm with a microplate reader.

Colony formation assay. MHCC97-H and HepG2 cells in the logarithmic phase were dispersed into single cells by trypsin digestion. Cell suspensions containing 1,000 cells were seeded in six-well plates with complete medium and the plates were incubated for two weeks. The medium was removed and the plates were washed twice with PBS, after which the cells were fixed with paraformaldehyde for 15 min and stained with crystal violet solution for 15 min at room temperature. After washing, the cells were air-dried and the number of colonies was calculated for each group.

Flow cytometry for cell apoptosis analysis. BBR-induced apoptosis in MHCC97-H and HepG2 cells was quantitatively determined by flow cytometry using the Annexin V-FITC apoptosis detection kit (Vazyme) and a flow cytometer (FACSCalibur; BD Biosciences). Briefly, after treatment with BBR for 24 h, cells were collected by using 0.25% trypsin and washed twice with cold PBS for 5 min, washed with PBS and incubated with Alexa 488 and propidium iodide (PI) for cellular staining at room temperature for 10 min in the dark. The stained cells were analyzed by Cell Quest acquisition software (version 3.3; BD Biosciences).

Wound healing assay. Wound healing assay was performed to evaluate the migration ability of cells. Cells were seeded 5×10^5 cells per well in 6-well plates and allowed to adhere for 24 h. Confluent monolayer cells were scratched using a 20 μl pipette tip and then washed three times with 1X PBS to clear cell debris and suspension cells. Medium containing 1% FBS and BBR (50-200 μM) was added and the cells were allowed to close the wound for 48 h. Images were acquired under an fluorescence microscope (Model DMi8, Leica Microsystems GmbH) at 0, 24 and 48 h at the same position of the wound (magnification, x10). The migration distance was calculated by the change in wound size during the 24 and 48 h period using Adobe Photoshop CS6 software (Adobe Systems, Inc.). The experiment was performed in triplicate.

Transwell assay. A 24-well Transwell plate (8-mm pore size; Corning, Inc.) was used to measure the migratory and invasive ability of each cell line. The inserts in the Transwell were coated with a thin layer of 0.25 mg/ml Matrigel Basement

Table I. Pharmacokinetic properties of berberine.

Name	OB (%)	DL	BBB	Caco-2	MW	TPSA	AlogP	Hdon	Hacc	FASA-
Berberine	36.86	0.78	0.57	1.24	336.39	40.80	3.45	0	4	0.19

OB, oral bioavailability; DL, drug-likeness; BBB, blood-brain barrier; Caco-2, Caco-2 permeability; MW, molecular weight (g/mol); TPSA, total polar surface area; AlogP, octanol-water partition coefficient; Hdon, H-bond donor; Hacc, H-bond acceptor; FASA-, fractional negative accessible surface area.

Membrane Matrix (BD Biosciences) at 37˚C for 30 min. MHCC97-H and HepG2 cells were treated with BBR for 24 h, trypsinized and seeded into the upper Transwell chamber ($2.5x10^4$ cells) in 100 μl of serum-free medium. Complete medium (600 μl) containing 10% FBS was added to the lower chamber. Triplicate wells were used for each group. The cells were allowed to migrate through the filters for 48 h at 37˚C in a humidified incubator with 5% CO_2. Cells attached to the lower surface of the membrane were fixed in 4% paraformaldehyde for 30 min and stained with 0.1% crystal violet at room temperature. The cells on the upper surface of the filters were removed by wiping with a cotton swab. The number of stained cells on the lower surface of the filters was counted at x20 magnification under a fluorescence microscope (Model DMi8; Leica Microsystems GmbH). A total of five fields of view were counted for each Transwell filter.

Statistical analysis. Data are presented as the mean ± SEM. All statistical analyses were performed with SPSS 19.0 statistical software (IBM Corp.). The data are expressed as the mean ± SEM. Statistical analysis was performed by one-way ANOVA followed by Tukey's multiple comparison test. Western blot analysis was repeated at least three times. $P<0.05$ was considered to indicate a statistically significant difference.

Results

Pharmacokinetic properties and putative targets of BBR. Pharmacokinetic properties play a vital role in drug discovery. Pharmacokinetic properties for BBR including Caco-2 permeability, DL, FASA-, OB, BBB and Lipinski's rule of five (MW, TPSA, AlogP, Hdon, Hacc) were obtained from TCMSP (Table I).

A total of 230 putative targets were predicted for BBR by TCMSP and PharmMapper, and duplicated potential targets were removed. Detailed information on candidate targets are provided in Table SI.

BBR-BBR targets network analysis. As shown in Fig. 2, a graph of BBR-BBR targets interaction was constructed based on 231 nodes (one compound and 230 candidate targets) and 230 edges. BBR-BBR targets network analysis displayed that BBR targeted proteins including AKT1, PTGS2, PDK2, MMP2, MMP8, CDK2, CDK6, CASP3, CASP1, ALB and GSK3B. Multiple targets predicted as hits for BBR in this network may be critical to the treatment of HCC. Previous research has shown MMP2 may act as an oncogene in HCC (31), and high expression of CDK2 may be more aggressive in HCC (32).

Identification of targets related to HCC. The present study identified 611 and 6,927 HCC-significant targets from OncoDB. HCC and Liverome, respectively. As displayed in Table SII, 167 candidate targets were obtained, and duplicated candidate targets were deleted.

In order to validate the molecular mechanisms of BBR acting on HCC, a PPI network analysis and a GO and pathway enrichment analysis on the common targets of BBR and HCC-significant targets were conducted.

PPI network of HCC-significant targets. The protein-protein interaction network of the common targets was constructed using the STRING database. Only one target did not show any protein-protein interactions, while two targets could not be found in the above database. A total of 164 nodes and 1,292 edges (Fig. 3) are shown in this network. In total, 12 genes, including *ALB, AKT1, SRC, IGF1, EGFR, HSP90AA1, ESR1, CASP3, F2, MAPK14, MMP9* and *PTGS2*, with degree ≥40, were selected as key genes. A large number of edges were obtained for each node (101 for *ALB*, 74 for *AKT1*, 62 for *SRC*, 57 for *IGF1*, 57 for *EGFR*, 56 for *HSP90AA1*, 53 for *ESR1*, 47 for *CASP3*, 44 for *F2*, 44 for *MAPK14*, 43 for *MMP9* and 41 for *PTGS2*). The results of the PPI network analysis revealed that these key genes may play important roles in the treatment of HCC.

GO and pathway enrichment analysis for target genes. To identify the biological function of the candidate targets, functional enrichment analysis was performed using DAVID database. The detailed results of GO terms and pathways are presented in Table SIII. GO analysis suggested that the cellular components were related to cytosol, extracellular exosome, mitochondrion, nucleoplasm, extracellular region, extracellular space, cytoplasm, mitochondrial matrix, focal adhesion and receptor complex (Fig. 4A).The biological processes in which the targets were involved were related to protein autophosphorylation, steroid hormone mediated signaling pathway, transcription initiation from RNA polymerase II promoter, response to drug, peptidyl-tyrosine phosphorylation, positive regulation of phosphatidylinositol 3-kinase signaling, positive regulation of ERK1 and ERK2 cascade, purine-containing compound salvage and intracellular receptor signaling pathway (Fig. 4B). The molecular function terms were associated with steroid hormone receptor activity, protein tyrosine kinase activity, drug binding, protein homodimerization activity, transmembrane receptor protein tyrosine kinase activity, ATP binding, enzyme binding, identical protein binding and steroid binding (Fig. 4C). These results suggested that these biological characteristics played a critical role in the treatment of HCC
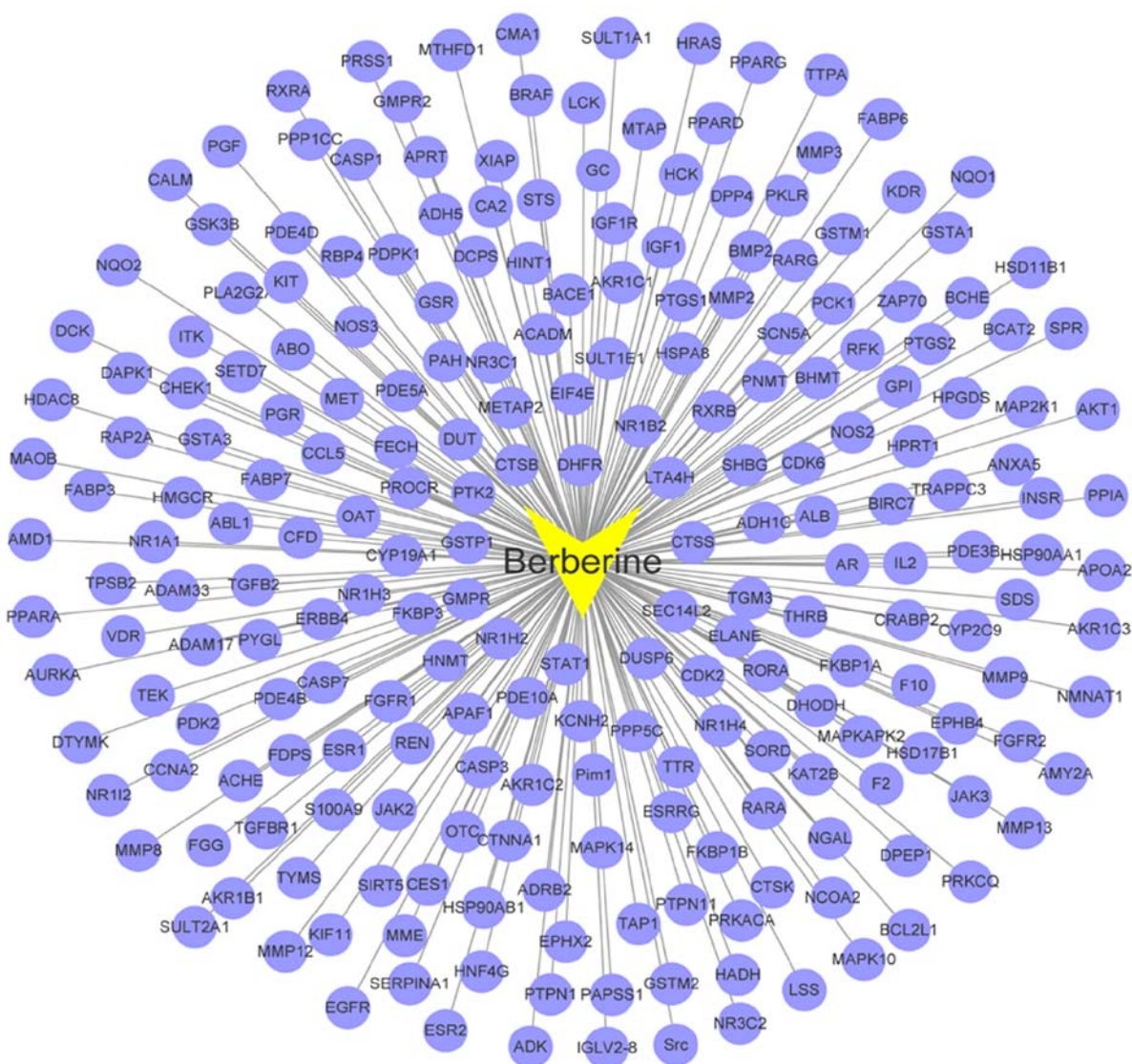
Figure 2. BBR-BBR targets network. The network consists of berberine and 230 berberine targets (Yellow V represents BBR, blue circles represent potential targets, and edges represent the relationships between BBR and potential BBR targets). BBR, berberine.
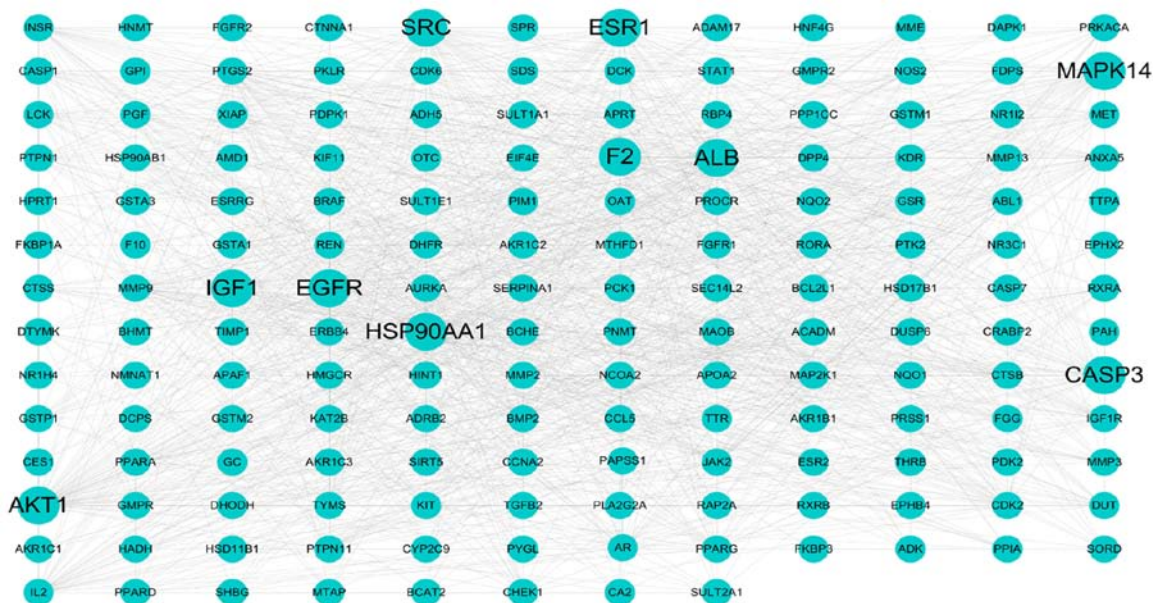

Figure 3. Protein-protein interaction network constructed using STRING. STRING, Search Tool for the Retrieval of Interacting Genes/Proteins.
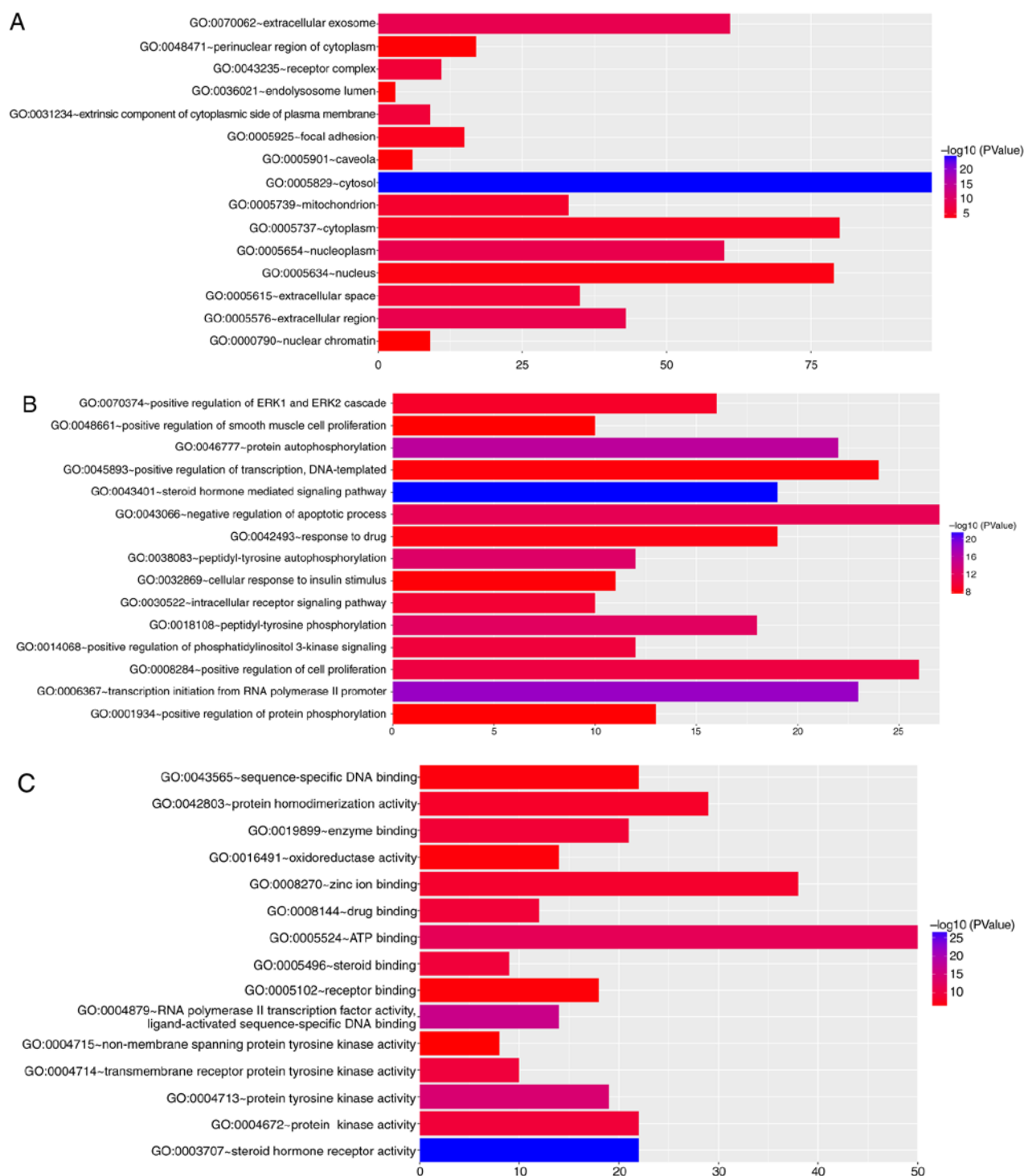
Figure 4. Enriched GO terms. The top 15 significantly enriched terms of the targets genes in (A) cellular component, (B) biological process and (C) molecular function. GO, gene ontology.

by BBR. Kyoto Encyclopedia of Genes and Genomes (KEGG) pathways indicated that pathways in cancer, PI3K-Akt signaling pathway, proteoglycans in cancer, prostate cancer, metabolism of xenobiotics by cytochrome P450, chemical carcinogenesis, small cell lung cancer, progesterone-mediated oocyte maturation, Ras signaling pathway and thyroid hormone signaling pathway, were involved in the therapy of HCC with BBR (Fig. 4D). Taken together, the above results showed that PI3K/AKT signaling pathway may potentially serve a key role in the BBR treatment process of HCC.

Docking of BBR to AKT. After applying the molecular docking approach according to the visual ligand-protein docking results, an *in silico* analysis was used to determine the binding site of BBR on AKT. The binding energy of BBR and AKT (PDB-ID:3MVH) was -8.83; BBR could be docked into the active site of AKT. Secondly, BBR was found to compete with ATP for the ATP-binding site of AKT, to which it bound tightly by forming hydrogen bonds with the backbone amino and carbonyl groups of the corresponding residues (Lys-158, Ala-230) and also by establishing hydrophobic contacts
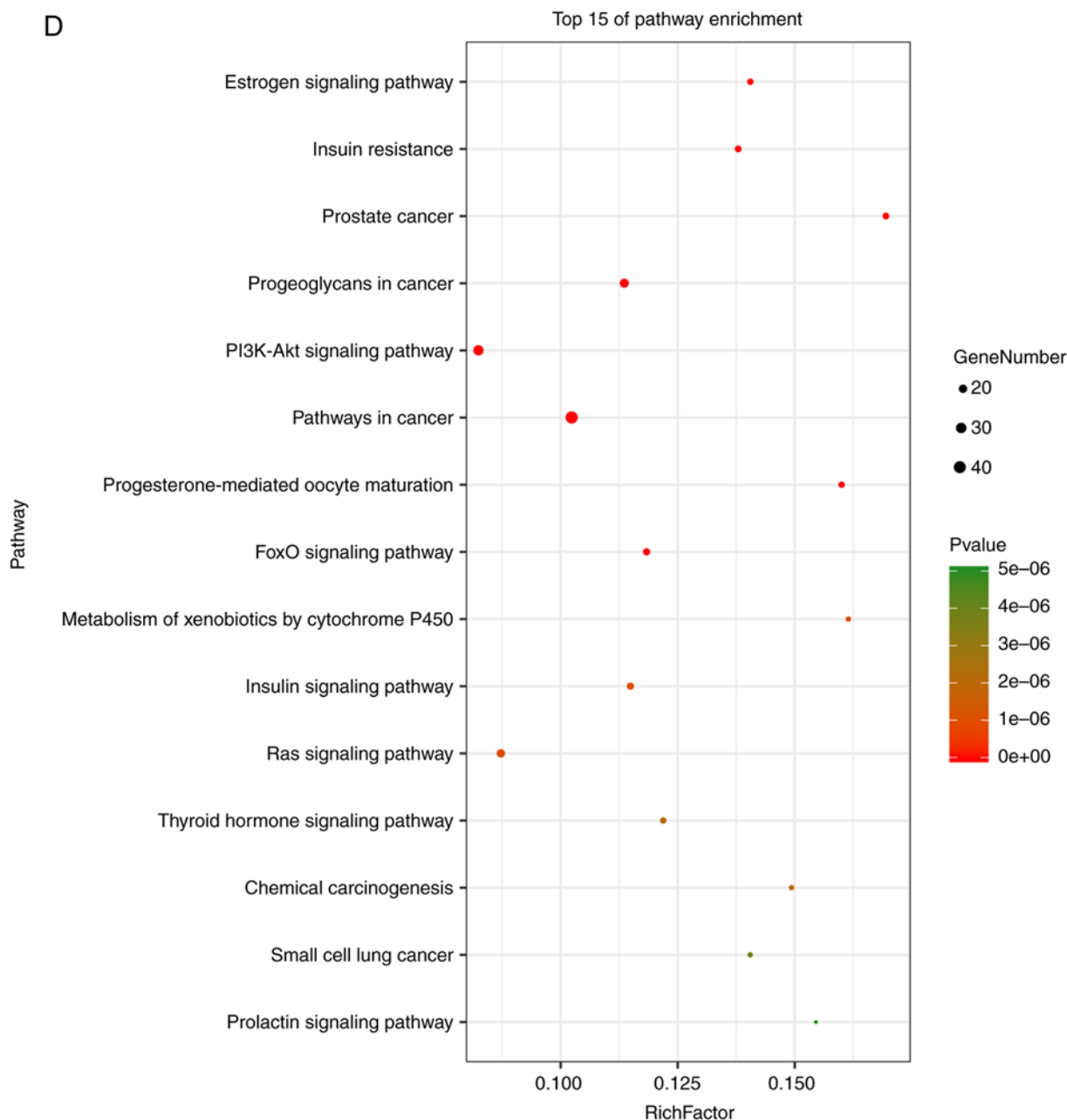
D

Figure 4. Continued. (D) Top 15 significantly pathways in pathway enrichment analysis for potential targets (P<0.05). GO, gene ontology.

(Gly-159, Gly-157, Leu-156, Val-164, Ala-177, Met-281, Tlu-211, Tlu-291, Tyr-229, Phe-438) with side chains of surrounding residues. The inhibitory activities were confirmed with molecular docking analysis when considering H-bond interaction, electrostatic potential energy, hydrophobic interaction of ligand molecules in the active pocket of AKT (Fig. 5). These results demonstrated that the binding of BBR to the active site of AKT could potentially suppress its activation, which could contribute to the inhibitory effects of BBR on proliferation and migration of HCC.

BBR inhibits cell growth and induces cell apoptosis of MHCC97-H and HepG2 cells. Viability and proliferation of MHCC97-H and HepG2 cells were assessed by MTT and colony formation assays, respectively. BBR treatment significantly inhibited the growth of MHCC97-H and HepG2 cells

(Fig. 6A) when treated BBR for 24 h. With the increase of concentration, the inhibition rate of cells increased significantly. Consistently, BBR decreased colony numbers of MHCC97-H and HepG2 cells at all indicated doses (Fig. 6B). These data suggested that the inhibitory effects of BBR could contribute to the suppression of HCC cell viability and proliferation. To further investigate the effect of BBR treatment on cell apoptosis, flowcytometry was performed using an Annexin V-FITC/PI kit. In the present study, both early (A-V-SP) and late (PI-SP) apoptotic cells were counted, as shown in the lower right and the upper right quadrant of the scatter plots, respectively. As demonstrated in Fig. 6C, after a 24-h treatment of HepG2 cells with BBR, the percentages of total apoptotic cells were: 4.2% (0 μM, vehicle treated control), 4.7% (50 μM), 5.6% (100 μM) and 16.9% (200 μM). For MHCC97-H cells, the percentages of total apoptotic cells
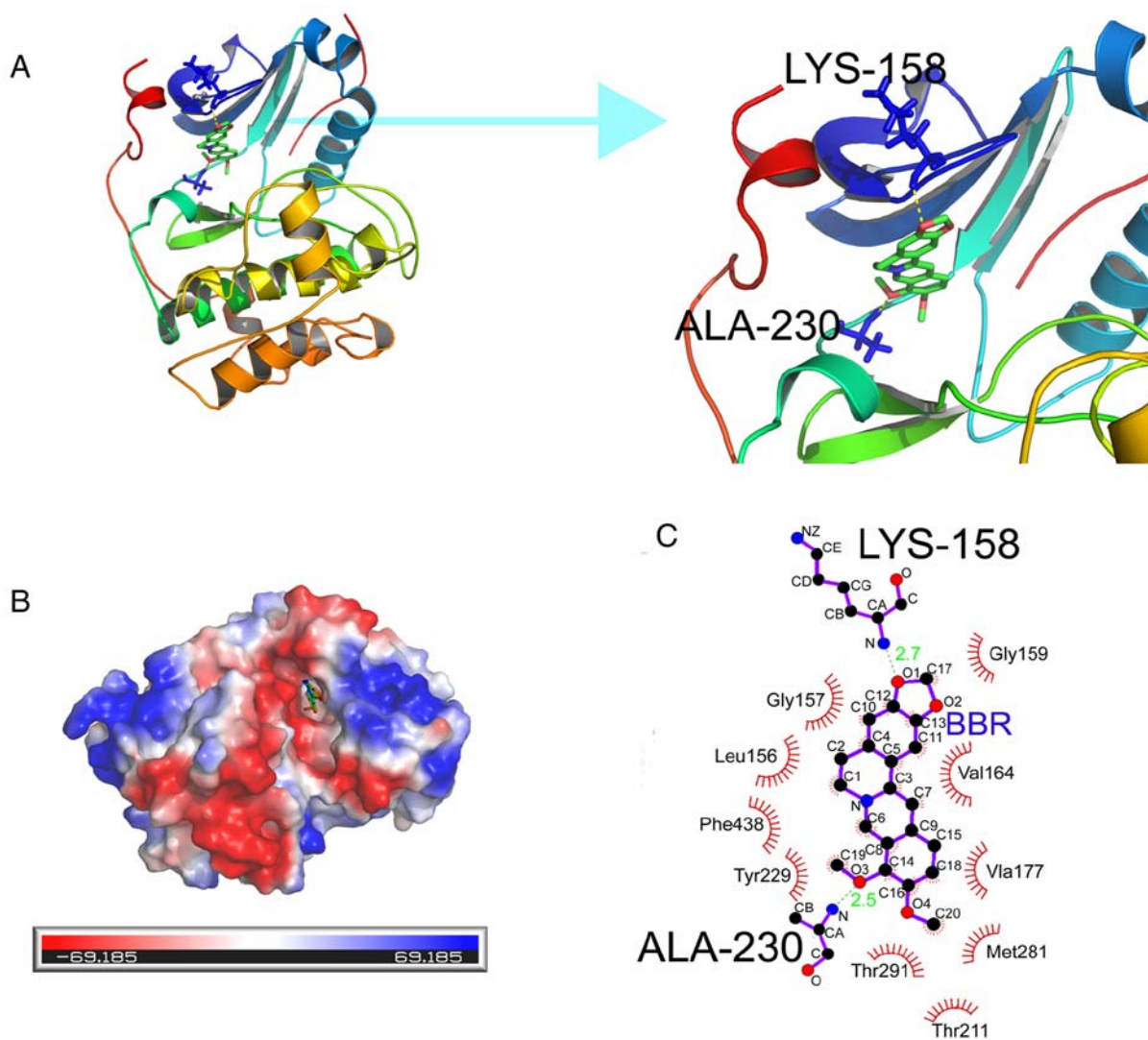
Figure 5. Ligand interaction and binding diagrams of BBR in the active site of AKT. (A) 3D interaction diagram obtained using PyMOL. BBR forms hydrogen bonds (Lys-158, Ala-230) with proteins. Hydrogen bond represented by yellow dashed line. (B) Electrostatic surfaces of BBR and AKT obtained using PyMOL. Lower electrostatic potential denotes better binding ability. BBR colored. (C) 2D schematic of interactions by ligplot. BBR, berberine.

were: 10% (0 μM, vehicle treated control), 11.8% (50 μM), 16% (100 μM) and 33% (200 μM).

BBR suppresses cell migration and invasion of MHCC97-H and HepG2 cells. As PI3K/AKT pathway plays a critical role in cancer cell migration, the effects of BBR on the invasion and migration ability of HCC cells were investigated. To this end, wound healing and Transwell chamber migration assays were performed *in vitro*. The relative migrated distance in BBR treated group was significantly smaller than that in the non-treated group, at indicated time points (P<0.05; n=3; Fig. 7A). Matrigel matrix invasion assay further indicated BBR treatment suppressed HCC cell migration (Fig. 7B).

BBR inhibits PI3K/AKT signaling pathway in HCC cells. To confirm the effect of BBR on PI3K/AKT signaling pathway, changes in PI3K/AKT effector proteins in HCC cells were analyzed by western blotting. As shown in Fig. 8, HCC cells possessed a high basal level of PI3K and p-AKT, indicating that HCC cells potentially rely on PI3K/AKT for proliferation and migration. However, BBR treatment significantly inhibited

the levels of PI3K and p-AKT without affecting the total AKT protein. Further, AKT phosphorylation was suppressed in a BBR concentration-dependent manner (Fig. 8). This implied a potential relationship between the inhibitory effects of BBR on cancer cell growth and migration and the suppression of the PI3K/AKT pathway.

Discussion

Over the past few decades, there has been a significant decline in the rate of novel phytochemicals that have been translated into effective drugs. Currently, the most important problem for novel drug development is a lack of therapeutic efficacy in clinical trials accounting for 33% of failures (33). Thus, to maximize drug efficacy in pharmaceutical development, network pharmacology has been recently introduced to analyze the biological network of drug candidates, in order to design poly-target phytochemicals. Previous studies have shown that BBR potentially represses tumor progression by inhibiting cell proliferation (34), inducing cell cycle arrest and cell death, in various cancer cells (35,36). In the present study,
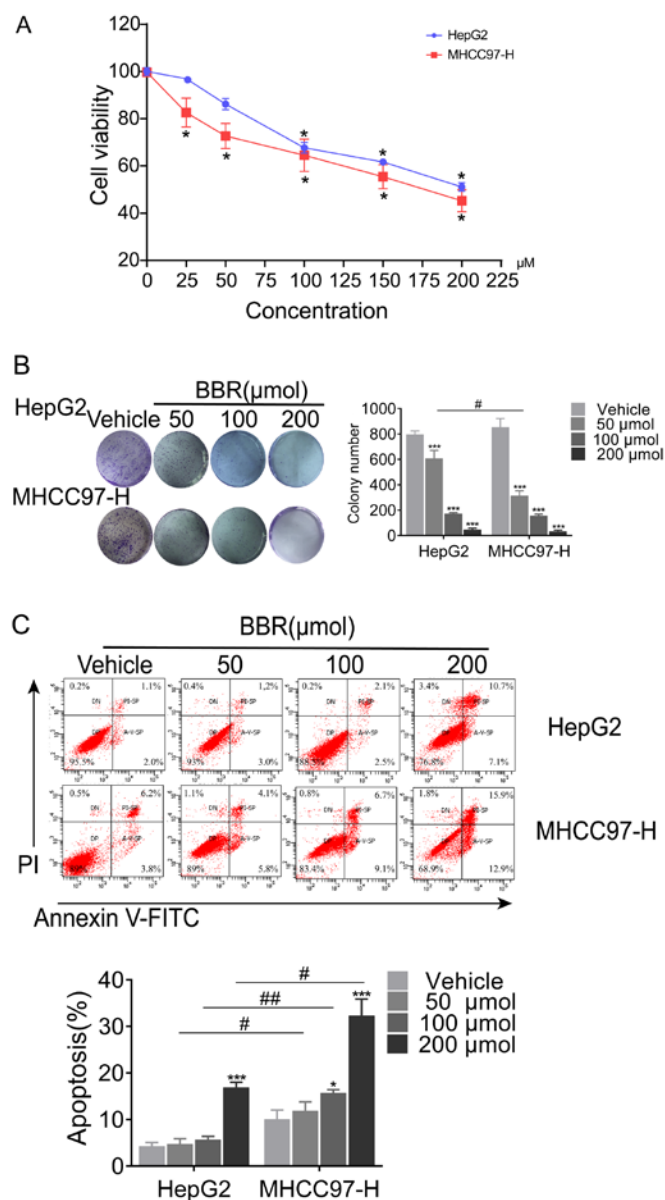
Figure 6. BBR decreases cell viability and induces cell apoptosis of MHCC97-H and HepG2 cells in a dose dependent manner. (A) MHCC97-H and HepG2 cells were treated with BBR at various concentrations for 24 h and processed for MTT assay. All data are presented as the mean ± standard error of mean (n=3), *P<0.05 vs. control group (non-berberine-treated) of the same cell line. (B) Colony formation assay was performed in MHCC97-H and HepG2 cells incubated with BBR. Histogram indicating the colony number of each group based on replicates of the colony formation assay (n=3). ***P<0.001 vs. the control group. #P<0.05. (C) HCC cells were treated with varying concentrations of BBR in complete medium for 24 h. Cell apoptosis was examined by flow cytometry using Annexin V/PI double staining following the manufacturer's protocol. The lower right quadrant of the FACS histograms indicates the percentage of early apoptotic cells and the upper right quadrant indicates the percentage of late apoptotic cells. The data are presented as mean ± standard error of mean (n=3). Significant difference vs. control group (non-berberine-treated), *P<0.05, ***P<0.001 vs. vehicle; #P<0.05 and ##P<0.01. BBR, berberine.
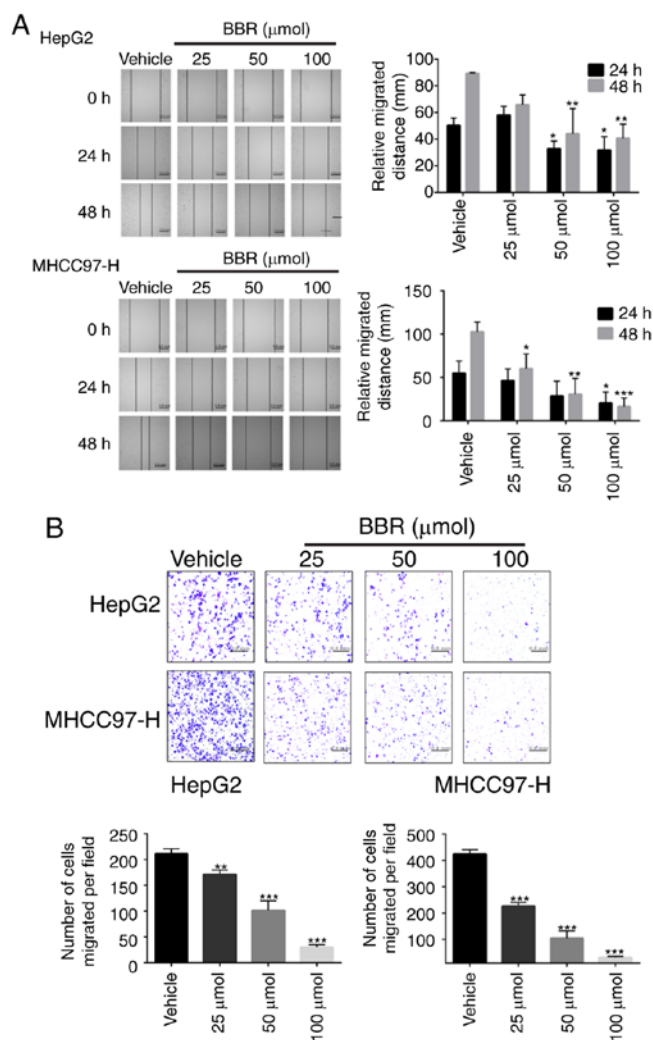

Figure 7. BBR inhibits invasion and migration of MHCC97-H and HepG2 cells in a dose-dependent manner. (A) Wound-healing assay for migration in cells. The scar closure area was detected by measuring the distance of the wound surface healing after treatment with BBR. (B) Following treatment, the cell invasion ability was significantly inhibited in a dose-dependent manner. All bar graphs are presented as mean ± standard error of mean (n=3). *P<0.05, **P<0.01 and ***P<0.001 vs. the control group. BBR, berberine.

PPI network analysis revealed that *AKT1*, *ALB*, *SRC*, *IGF1*, *EGFR*, *HSP90AA1*, *ESR1*, *CASP3*, *F2*, *MAPK14*, *MMP9* and *PTGS2* could be the key genes that are essential for the survival of HCC. Pathway analysis elucidated that PI3K/AKT signaling pathway in cancer may be closely related to the progress of HCC. The present study hypothesized that BBR potentially

suppresses HCC progression by regulating AKT, based on the network pharmacology study results.

AKT is a serine-threonine kinase and a vital component of the PI3K/AKT/mammalian target of rapamycin signaling pathway. It is over-expressed in most types of cancer (37). Activated AKT phosphorylates downstream signaling molecules such as GSK3β, PRAS40, BAD and p70S6K, that promote survival, proliferation, growth and metastasis of cancer cells (38). Due to its central role in these pathways, inhibition of AKT is an attractive intervention strategy for the treatment of cancer (39). In the present study, the docking approach indicated that the binding potential between BBR and AKT (RAC-α serine/threonine-protein kinase) could lead to suppression of AKT activity. The inhibitory effect of BBR on PI3K/AKT pathway in HCC was validated and it was found that BBR could downregulate the expressions of p-AKT and PI3K in MHCC97-H and HepG2 cells, which could then inhibit the growth, cell migration and invasion of MHCC97-H and HepG2 cells in a dose-dependent manner. In addition, AKT pathway inhibition
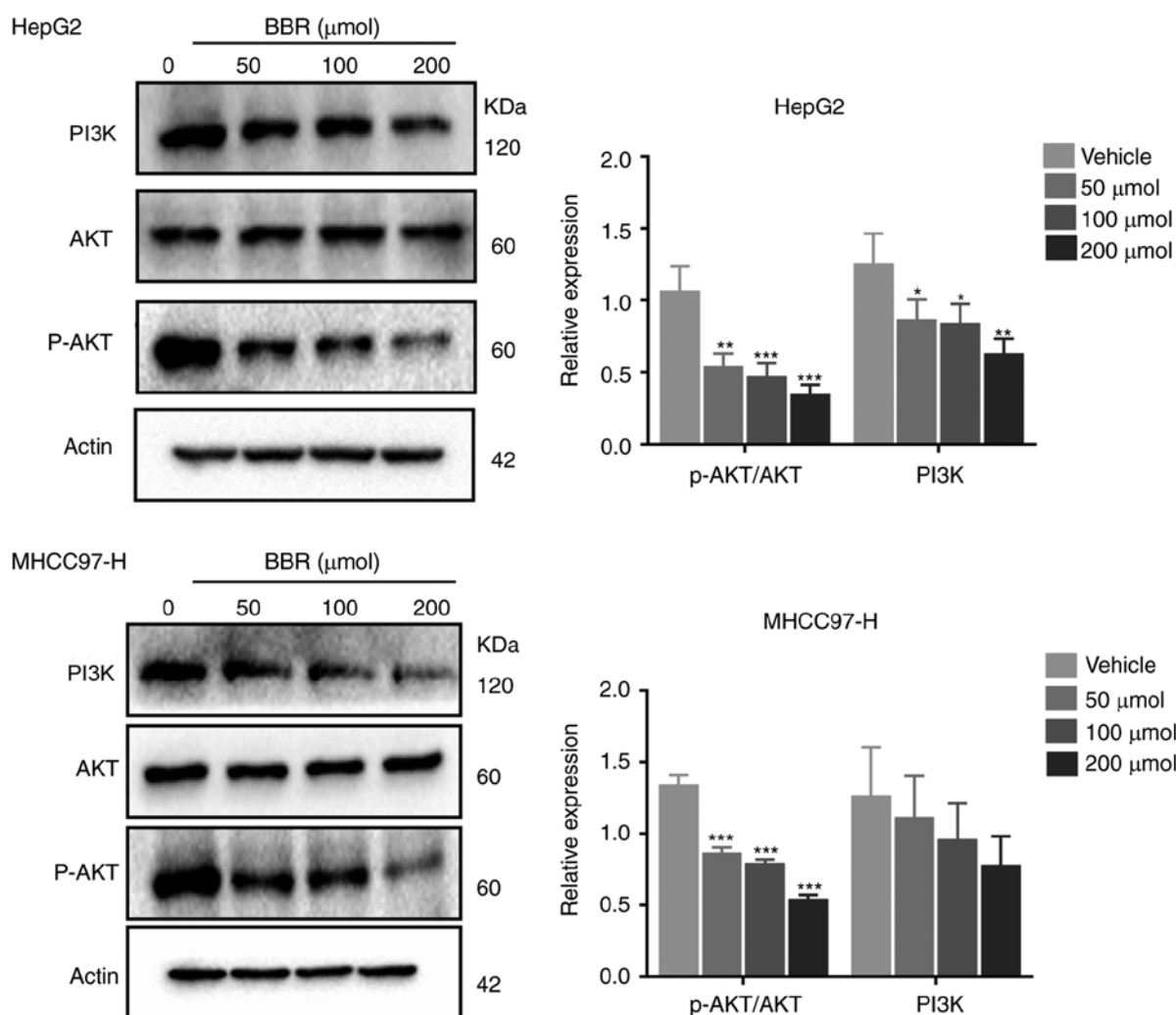
Figure 8. Inhibitory effects of BBR on protein expressions phosphorylation p-AKT/AKT in HCC cell lines. MHCC97-H and HepG2 cells were treated with vehicle or BBR at indicated concentrations for 24 h. Data are presented as the mean ± standard error of mean (n=3), $^*P<0.05$, $^{**}P<0.01$ and $^{***}P<0.001$ vs. control group. BBR, berberine.

by BBR also contributed to cell apoptosis in MHCC97-H and HepG2 cells. Based the current study, 100 μM is the ideal concentration of BBR in potential treatment. However, there are some limitations in the present study. For example, a lack of caspase inhibition experiment, which may also be relevant for the anti-HCC mechanism. In the future, further systematic and in-depth studies investigating the mechanism of anti-HCC will be conducted. In conclusion, the use of BBR as a sensitizer of cancer cells to AKT inhibitors should be further explored by *in vivo* experiments and in preclinical studies.

Acknowledgements

Not applicable.

Funding

Availability of data and materials

The analyzed data sets generated during the present study are available from the corresponding author on reasonable request.

Authors' contributions

LS, YL and XW contributed to experimental study, data analysis and drafted the manuscript. MMA, HP, WL and YL participated in the experiments. MH and QW designed and supervised all aspects of the study. All authors critically reviewed and revised the manuscript and approved the final manuscript as submitted.

Ethics approval and consent to participate

Not applicable.

Patient consent for publication

Not applicable.

Competing interests

The authors declare that they have no competing interests.

References

1. Bosch FX, Ribes J, Díaz M and Cléries R: Primary liver cancer: Worldwide incidence and trends. Gastroenterology 127 (Suppl 1): S5-S16, 2004.
2. Pisani P, Parkin DM, Bray F and Ferlay J: Estimates of the world-wide mortality from 25 cancers in 1990. Int J Cancer 83: 18-29, 1999.
3. Bray F, Ferlay J, Soerjomataram I, Siegel RL, Torre LA and Jemal A: Global cancer statistics 2018: GLOBOCAN estimates of incidence and mortality worldwide for 36 cancers in 185 countries. CA Cancer J Clin 68: 394-424, 2018.
4. Bruix J, Gores GJ and Mazzaferro V: Hepatocellular carcinoma: Clinical frontiers and perspectives. Gut 63: 844-855, 2014.
5. Pinter M and Peck-Radosavljevic M: Review article: Systemic treatment of hepatocellular carcinoma. Aliment Pharm Ther 48: 598-609, 2018.
6. Abdel-Rahman O and Lamarca A: Development of sorafenib-related side effects in patients diagnosed with advanced hepatocellular carcinoma treated with sorafenib: A systematic-review and meta-analysis of the impact on survival. Expert Rev Gastroenterol Hepatol 11: 75-83, 2017.
7. Imenshahidi M and Hosseinzadeh H: Berberis vulgaris and berberine: An update review. Phytother Res 30: 1745-1764, 2016.
8. Zhang Y, Wang X, Sha S, Liang S, Zhao L, Liu L, Chai N, Wang H and Wu K: Berberine increases the expression of NHE3 and AQP4 in sennosideA-induced diarrhoea model. Fitoterapia 83: 1014-1022, 2012.
9. Liu Y, Yu H, Zhang C, Cheng Y, Hu L, Meng X and Zhao Y: Protective effects of berberine on radiation-induced lung injury via intercellular adhesion molecular-1 and transforming growth factor-beta-1 in patients with lung cancer. Eur J Cancer 44: 2425-2432, 2008.
10. Rezaeiamiri E, Bahramsoltani R and Rahimi R: Plant-derived natural agents as dietary supplements for the regulation of glyco-sylated hemoglobin: A review of clinical trials. Clin Nutr: Feb 10, 2019 (Epub ahead of print). doi: 10.1016/j.clnu.2019.02.006.
11. Tillhon M, Guamán Ortiz LM, Lombardi P and Scovassi AI: Berberine: New perspectives for old remedies. Biochem Pharmacol 84: 1260-1267, 2012.
12. Jin P, Zhang C and Li N: Berberine exhibits antitumor effects in human ovarian cancer cells. Anticancer Agents Med Chem 15: 511-516, 2015.
13. Pierpaoli E, Arcamone AG, Buzzetti F, Lombardi P, Salvatore C and Provinciali M: Antitumor effect of novel berberine derivatives in breast cancer cells. Biofactors 39: 672-679, 2013.
14. Li CH, Wu DF, Ding H, Zhao Y, Zhou KY and Xu DE: Berberine hydrochloride impact on physiological processes and modulation of twist levels in nasopharyngeal carcinoma CNE-1 cells. Asian Pac J Cancer Prev 15: 1851-1857, 2014.
15. Li L, Wang X, Sharvan R, Gao J and Qu S: Berberine could inhibit thyroid carcinoma cells by inducing mitochondrial apoptosis, G0/G1 cell cycle arrest and suppressing migration via PI3K-AKT and MAPK signaling pathways. Biomed Pharmacother 95: 1225-1231, 2017.
16. Zhang Q, Zhang C, Yang X, Yang B, Wang J, Kang Y, Wang Z, Li D, Huang G, Ma Z, et al: Berberine inhibits the expression of hypoxia induction factor-1alpha and increases the radiosensi-tivity of prostate cancer. Diagn Pathol 9: 98, 2014.
17. Kou Y, Li L, Li H, Tan Y, Li B, Wang K and Du B: Berberine suppressed epithelial mesenchymal transition through cross-talk regulation of PI3K/AKT and RARα/RARβ in melanoma cells. Biochem Biophys Res Commun 479: 290-296, 2016.
18. Guo P, Cai C, Wu X, Fan X, Huang W, Zhou J, Wu Q, Huang Y, Zhao W, Zhang F, et al: An insight into the molecular mechanism of berberine towards multiple cancer types through systems pharmacology. Front Pharmacol 10: 857, 2019.
19. Hao DC and Xiao PG: Network pharmacology: A Rosetta stone for traditional Chinese medicine. Drug Develop Res 75: 299-312, 2014.
20. Zoete V, Grosdidier A and Michielin O: Docking, virtual high throughput screening and in silico fragment-based drug design. J Cell Mol Med 13: 238-248, 2009.
21. Ru J, Li P, Wang J, Zhou W, Li B, Huang C, Li P, Guo Z, Tao W, Yang Y, et al: TCMSP: A database of systems pharmacology for drug discovery from herbal medicines. J Cheminform 6: 13, 2014.
22. Liu X, Ouyang S, Yu B, Liu Y, Huang K, Gong J, Zheng S, Li Z, Li H and Jiang H: PharmMapper server: A web server for potential drug target identification using pharmacophore mapping approach. Nucleic Acids Res 38: W609-W614, 2010.
23. Yu H, Chen J, Xu X, Li Y, Zhao H, Fang Y, Li X, Zhou W, Wang W and Wang Y: A systematic prediction of multiple drug-target interactions from chemical, genomic and pharmacological data. PLoS One 7: e37608, 2012.
24. Su WH, Chao CC, Yeh SH, Chen DS, Chen PJ and Jou YS: OncoDB.HCC: An integrated oncogenomic database of hepatocellular carcinoma revealed aberrant cancer target genes and loci. Nucleic Acids Res 35: D727-D731, 2007.
25. Szklarczyk D, Franceschini A, Wyder S, Forslund K, Heller D, Huerta-Cepas J, Simonovic M, Roth A, Santos A, Tsafou KP, et al: STRING v10: Protein-protein interaction networks, integrated over the tree of life. Nucleic Acids Res 43: D447-D452, 2015.
26. Huang DW, Sherman BT and Lempicki RA: Systematic and integrative analysis of large gene lists using DAVID bioinformatics resources. Nat Protoc 4: 44-57, 2009.
27. Huang DW, Sherman BT and Lempicki RA: Bioinformatics enrichment tools: Paths toward the comprehensive functional analysis of large gene lists. Nucleic Acids Res 37: 1-13, 2009.
28. Szklarczyk D, Morris JH, Cook H, Kuhn M, Wyder S, Simonovic M, Santos A, Doncheva NT, Roth A, Bork P, et al: The STRING database in 2017: Quality-controlled protein-protein association networks, made broadly accessible. Nucleic Acids Res 45: D362-D368, 2017.
29. Chuang CH, Cheng TC, Leu YL, Chuang KH, Tzou SC and Chen CS: Discovery of Akt kinase inhibitors through Structure-Based virtual screening and their evaluation as potential anticancer agents. Int J Mol Sci 16: 3202-3212, 2015.
30. Renata DP, Christian VQ, Ruiz DD, Gargano F and de Souza ON: A selective method for optimizing ensemble docking-based experiments on an InhA Fully-Flexible receptor model. BMC Bioinformatics 19: 235, 2018.
31. Liu J, Li X, Huang J and Liu Y: Matrix metalloproteinase 2 knockdown suppresses the proliferation of HepG2 and Huh7 cells and enhances the cisplatin effect. Open Med (Wars) 14: 384-391, 2019.
32. Xu C, Zhang W, Zhang X, Zhou D, Qu L, Liu J, Xiao M, Ni R, Jiang F, Ni W and Lu C: Coupling function of cyclin-dependent kinase 2 and Septin2 in the promotion of hepatocellular carcinoma. Cancer Sci 110: 540-549, 2019.
33. Hong M, Li S, Wang N, Tan HY, Cheung F and Feng Y: A biomedical investigation of the hepatoprotective effect of radix salviae miltiorrhizae and network Pharmacology-Based prediction of the active compounds and molecular targets. Int J Mol Sci 18: E620, 2017.
34. Hong M, Li S, Tan H, Cheung F, Wang N, Huang J and Feng Y: A Network-Based pharmacology study of the Herb-induced liver injury potential of traditional hepatoprotective Chinese herbal medicines. Molecules 22: E632, 2017.
35. Wang X, Wang N, Li H, Liu M, Cao F, Yu X, Zhang J, Tan Y, Xiang L and Feng Y: Up-Regulation of PAI-1 and Down-regulation of uPA are involved in suppression of invasive-ness and motility of hepatocellular carcinoma cells by a natural compound berberine. Int J Mol Sci 17: 577, 2016.
36. Wang N, Feng Y, Zhu M, Tsang CM, Man K, Tong Y and Tsao SW: Berberine induces autophagic cell death and mitochondrial apoptosis in liver cancer cells: The cellular mechanism. J Cell Biochem 111: 1426-1436, 2010.
37. Cantley LC and Neel BG: New insights into tumor suppression: PTEN suppresses tumor formation by restraining the phosphoinositide 3-kinase/AKT pathway. Proc Natl Acad Sci USA 96: 4240-4245, 1999.
38. Manning BD and Toker A: AKT/PKB signaling: Navigating the network. Cell 169: 381-405, 2017.
39. Courtney KD, Corcoran RB and Engelman JA: The PI3K pathway as drug target in human cancer. J Clin Oncol 28: 1075-1083, 2010.